Volume 73 • Issue 1 • November 2015

Journal of Achievements in Materials and Manufacturing Engineering

International Scientific Journal published monthly by the World Academy of Materials and Manufacturing Engineering

Structure and properties of amorphous and nanocrystalline $Fe_{78}Si_{11-x}B_{11}Y_x$ (x = 0 or 2) alloys produced in a single production step using controlled parameters melt-spinning method

K. Błoch*

Institute of Physics, Faculty of Materials Processing Technology and Applied Physics
Czestochowa University of Technology, Al. Armii Krajowej 19, 42-200 Częstochowa, Poland
Corresponding e-mail address: 23kasia1@wp.pl

ABSTRACT

Purpose: The paper presents results of structural and magnetic properties of $Fe_{78}Si_{11}B_{11}$ and $Fe_{78}Si_9B_{11}Y_2$ alloys in the form of ribbons. The effect of addition of yttrium on the structure and magnetic properties was investigated.

Design/methodology/approach: The investigated samples were prepared in the form of ribbons using the melt-spinning method. The material structures were investigated using X-ray diffractometry, Mössbauer spectroscopy and scanning electron microscopy. The magnetic properties were studied using using vibrating magnetometer.

Findings: Samples were fabricated using rapid cooling at a rotating copper wheel. Images of fractures of investigated samples obtained by decohesion using same magnifications are similar. The distinct vein like structure or the husk structure are not visible thought they are typical of amorphous and nanocrystalline materials with a high degree of internal stress. Mössbauer spectrum is typical as for amorphous materials that are ferromagnetic. It consists of six lines forming a Zemman's sextet. The hyperfine induction field distribution obtained for this sample shows clearly separated two components: low- and high-field. After the introduction of 2% at. Y to the alloy $Fe_{78}Si_{11}B_{11}$ in place of Si partial crystallization occurred. The shape of the initial magnetization curves is similar and corresponds to materials with low effective anisotropy.

Originality/value: The paper presents some researches of the Fe-based bulk amorphous alloys obtained by the melt-spinning method

Keywords: Amorphous alloy; Nanocrystalline alloy; Structure; Microstructure; Hysteresis loops

Reference to this paper should be given in the following way:

K. Błoch, Structure and properties of amorphous and nanocrystalline $Fe_{78}Si_{11-x}B_{11}Y_x$ (x = 0 or 2) alloys produced in a single production step using controlled parameters melt-spinning method, Journal of Achievements in Materials and Manufacturing Engineering 73/1 (2015) 5-12.

MATERIALS

1. Introduction

In the present age, the most desirable and necessary for the further development of civilization medium is electrical current. Therefore, research into reducing its consumption and the reduction of losses during transmission are carried out within the best scientific centers and research institutions. In addition, they are also carried out research on developing new electrical goods, which in itself will show better properties than commercially applicable FeSi transformer sheets or copper wires [1-3]. There is no need to cite examples of where devices use mains electricity or modern-powered portable consumer electronics batteries. In the last half-century, many new groups of materials for use in electrical engineering and electronics were developed. One of the most promising groups of solid materials are amorphous and nanocrystalline alloys [4-7]. Such alloys are extensively studied to this day and apart from exceptional magnetic properties they also exhibit unique mechanical properties [8-14]. The first of these materials were taken in the '60 of XX century in the form of thin layers made by the process of evaporation [15]. However, their use has not been possible on a large scale because of the impossibility of forming and small volume. A method giving the opportunity to produce a solid sample free from surface medium and greater thickness was searched. As the author of this method for producing such samples H.S. Chen is considered [16]. He developed together with his colleagues unique method for its time involving the injection of liquified material on copper wheel rotating liquid metal stream. This method which is based on a simple apparatus is used to this day. The liquid metal stream solidified on the copper wheel with speed 10^4-10^6 K/s [17-19]. The product obtained by this method generally has the shape of a tape or flakes of a thickness not exceeding 100 mm [20-21]. Diagram showing the method of manufacturing amorphous strips are provided in Fig. 1.

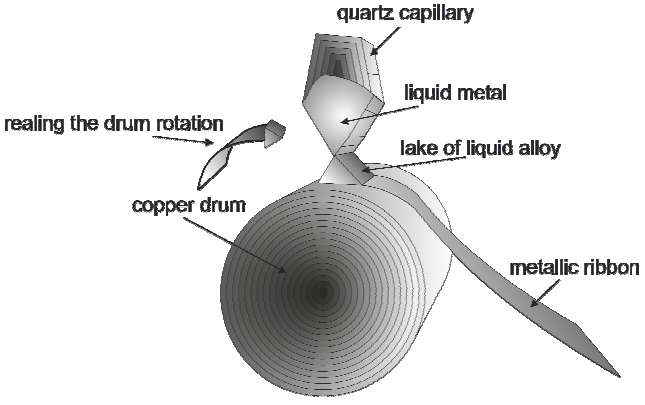

Fig. 1. The diagram showing the melt-spinning method [22]

The liquid melt is cooled unidirectionally, which generates a different surface topography on both sides. Due to obtained such a high cooling rate, it was possible to produce samples without crystallization process during solidification. The transition from liquid to solid state taking into account the glass transition temperature can be characterized by TCP curve, which is shown in Fig. 2.

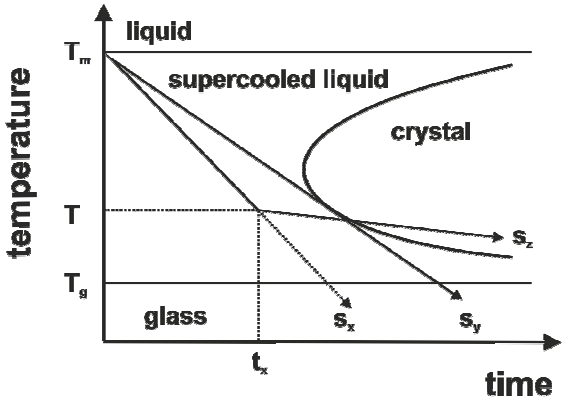

Fig. 2. A schematic curve TCP describing the devitrification process: S_x – the cooling rate of the liquid alloy on the drum, S_z – the cooling rate of the ribbon in the air, S_y – the critical cooling rate of a liquid, which achieves glass, t_x – cooling time of liquid metal, T_g – glass transition temperature, T_m – superheat temperature of the alloy.

A schematic TCP curve (Fig. 2) that describes the glass transition and the cooling curve of the liquid at a rate (S_x) substantially greater than the critical and the cooling time dependent on position of the TCP curve. If the cooling time of the strip on the outside side of the wheel would be too small to reduce the melt temperature below the temperature (T_g) then in the further ribbon would be cooled in air at a rate of (W), which is not capable of providing an amorphous state. This is shown in Fig. 2. Clearly it shows that devitrification liquid injected under argon pressure the melt is possible, when cooling time and cooling rate of this alloy, when the band leaves the surface of the copper wheel, allows to maintain the final temperature exceeding the glass transition temperature (T_g). The obtained alloys using the method of unidirectional cooling of the melt on a rotating copper wheel were characterized by amorphous structure, which in the case of alloys for use in electrical was then unacceptable. It was believed that because the magnetic properties and in particular the so-called soft magnetic properties are closely related to the crystal structure, for which it was believed that there is only a magnetic hysteresis loop. That misconception presented by Fisher and Koopman, when they watched magnetic

hysteresis loops for applied layers of Co-P, despite the absence of diffraction peaks for these compounds [23]. This belief was so strong that they didn't include examinations for amorphous materials, despite the very promising results. It was not until in 1960 Russian physicist Gubanow showed theoretically that the ferromagnetic order is not closely related to the crystal lattice [24]. This date is considered to be the beginning of modern group of electrotechnical materials, which are amorphous alloys. Such materials exhibit a high saturation magnetization, low losses on remagnetization and almost zero magnetostriction [25-26]. It was thought that those materials will alternate textured metal transformer cores and components for transformers and chokes. The conviction that lasted more than 20 years until the Japanese led by Suzuki presented to the world a different group of materials called nanocrystalline materials [27]. Suzuki has shown that properly performed procedure for heat treatment of amorphous alloys leads to nanocrystallization [28]. Those observations made up for his first patent [27] for nanocrystalline materials use in electrical engineering. Since then an intensive research on these materials began, and methods of their obtaining [29-31]. Generally, it is assumed that nanocrystalline materials are produced by annealing of the amorphous materials [32-34]. Annealing process itself is fairly simple, but its design requires a series of preliminary studies and trials. The most common method is that proposed by Suzuki et al. This method consists of long-term annealing at a temperature well below the crystallization temperature. This process lasts a long time and is energy consumable. Another method of heat treatment is a short annealing at a temperature near crystallization. However, the reproducibility in preparation of crystallites of similar size is quite small. The basis for carrying out these thermal treatments is to know the value of the crystallization temperature (T_x), which is determined on the basis of an analysis of the heat flow curve as a function of temperature. Differential calorimetry curves give much more information that allow to describe the thermal stability of amorphous alloys and how they crystallization. For a complete description of the thermal stability of the amorphous alloy should specify the glass transition temperature (T_g), the temperature of the beginning of the crystallization (T_x), the peak temperature (T_l), a softening temperature of the melt (T_m) and melt temperature (T_l). Knowing these temperatures can be determined: the supercooled liquid temperature range $\Delta T_x = T_x - T_g$ [35-39], reduced glass transition temperature $T_{rg} = T_g/T_m$ [35, 40] and $T_{rg} = T_g/T_l$, ΔT_m The temperature range determined from the difference ($= T_l - T_m$) [35], the temperature of supercooling $\Delta T_l = T_l - T_x$ [43], the modified parameter ability to form glassy state (GFA) γ_m ($= (2T_x - T_g)/T_l$) [47], parameter $\gamma = T_x/(T_g + T_l)$ [35] and parameter δ ($= T_x/(T_l - T_g)$) [43]. A completely different method of heat treatment which does not require knowledge of the above-mentioned temperatures and giving great hope to thermal processing method is the so-called impulse nanocrystallization [41]. It involves annealing the amorphous sample at temperatures well above the crystallization temperature, but for a very short period of time amounting to fractions of a second. The author of this nanocrystallization method considered to T. Kulik from Warsaw University of Technology. However, any of the above methods requires at least one further treatment cycle in addition to the production process. There is, however, possible to fabricate nano-material in the form of a tape in a single production step [42]. To further characterize it the impact of three key parameters occurring in the manufacture of tapes must be determined: the pressure that propels the liquid alloy on copper wheel, the linear velocity of the copper cylinder gap at the bottom of the crucible. A diagram for describing change in rotation speed of the copper wheel as a function of pressure is shown in Fig. 3.

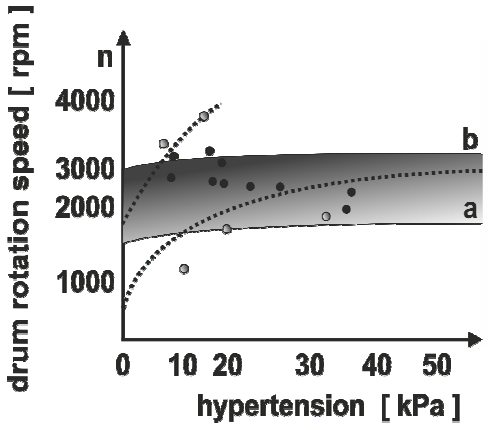

Fig. 3. Changing the rotation speed of the copper cylinder as a function of hypertension

Boundary lines secreting area in Fig. 3 are selected from [43], and the dashed lines based on [44]. Such studies were conducted in Institute of Materials Science and Engineering of Warsaw University of Technology and the results are shown in Fig. 3. Black circles define the parameters for which it tapes of amorphous structure are done, and white space where you do not manage to obtain a spin glasses. The experiment was performed for constant linear velocity of the copper wheel (v = 32 m/s), the set temperature of heated alloy (T_m = 1200°) and the same diameter of the slots in a quartz capillary (0.22 mm). This means that the argon pressure of the ejecting molten alloy

to the rotating copper wheel is not important to the thickness of the obtained tapes. Using this experiment, you can plan the production of nanocrystalline materials, which are marked on the diagram 3 as grey circles.

The paper presents results of structural and magnetic properties for amorphous and nanocrystalline alloy strip produced using the method of melt-spinning.

2. Materials and methodology

The studied materials were produced in the form of thin ribbons of 3 mm width and 20 μm thickness using a melt-spinning method. The microstructure and structure of the alloy were investigated by means of X-ray diffractometry and electron scanning microscopy. The structure of tapes was examined using the BRUKER X-ray diffractometer, model ADVANCE D8. Investigations were carried out over the 2Θ range from 30° to 120°, with a measurement step of 0.02° and time per step of 5 s. Images of the material surface were obtained using a Zeiss SUPRA 35' high-resolution scanning electron microscope, utilizing the detection of secondary electrons (SE) and with an acceleration voltage of 25 kV. The structure of alloys was also studied using Mössbauer spectroscopy using POLON equipment. Those measurements employed Mössbauer ^{57}Co source. The use of NORMOS software for Mössbauer spectra analysis allowed to obtain distributions of hyperfine fields induction at the ^{57}Fe nuclei. The initial magnetization curves were measured in the range up to 2T, using vibrating sample magnetometer.

3. Results and discussion

Fig. 4 shows the fracture surface images of investigated samples.

Images of fractures of investigated samples obtained by decohesion using same magnifications are similar. The distinct vein like structure or the husk structure are not visible thought they are typical of amorphous and nanocrystalline materials with a high degree of internal stress. Only the smooth structure is visible, which means that the tested alloys were well relaxed after the manufacturing process. The addition of Yttrium in place of 2 at.% Si resulted in the partial crystallization of the alloy. Grains established for FeSiBY alloy sample are characterized by a nanoscale dimensions. Nanocrystallization of material was revealed by Mössbauer study. In Fig. 5 Mössbauer spectra is shown and the resulting distribution of the hyperfine induction field at the nuclei of ^{57}Fe.

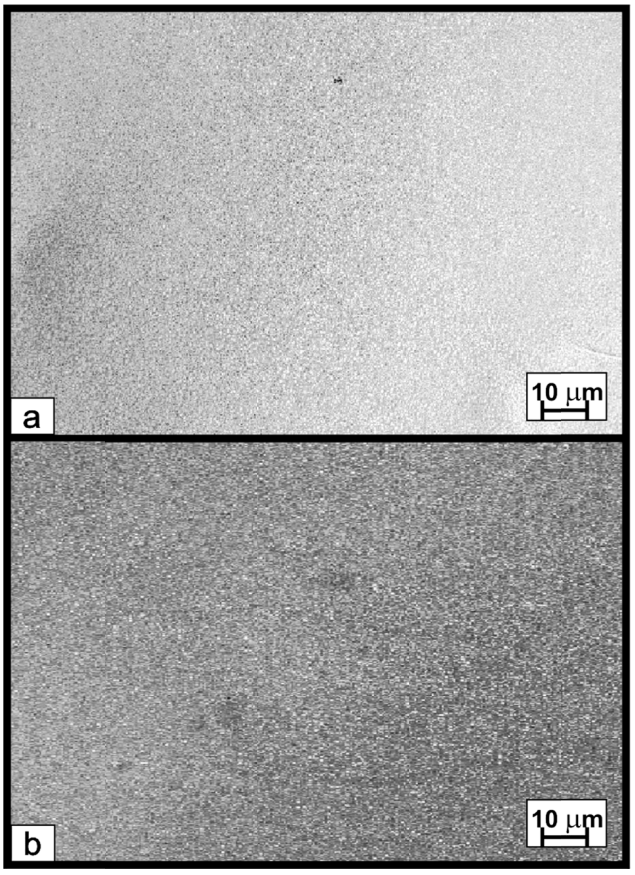

Fig. 4. SEM images of breakthroughs obtained for investigated samples of alloys: a) FeSiB and b) FeSi

Shown in Figure 5 Mössbauer spectrum is typical as for amorphous materials that are ferromagnetic. It consists of six lines forming a Zemman's sextet. The hyperfine induction field distribution obtained for this sample shows clearly separated two components: low- and high-field. This type of distribution is characteristic of metastable amorphous alloys, in which there are regions having different concentrations of iron. After the introduction of 2% at. Y to the alloy $Fe_{78}Si_{11}B_{11}$ in place of Si partial crystallization occurred. The result of this partial crystallization is emergence in the alloy volume of fine crystallites. Formed crystalline phase is paramagnetic phase described by a single line. The remainder of the hyperfine induction field distribution is similar to that observed for the $Fe_{78}Si_{11}B_{11}$ alloy sample. The percentage of paramagnetic crystalline phase is around 13% relative to the volume of the alloy.

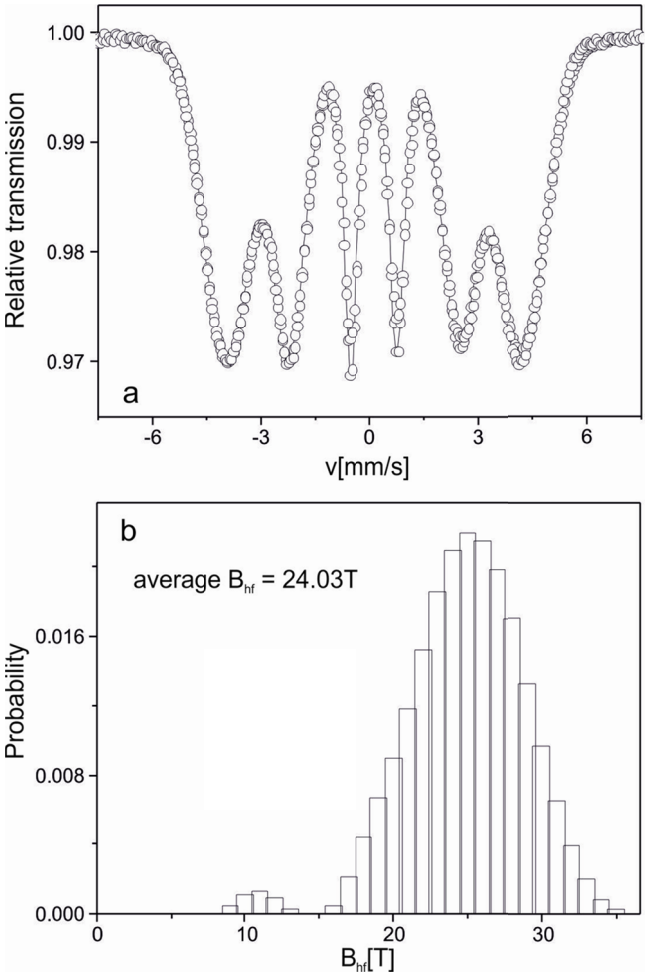

Fig. 5. The transmission Mössbauer spectra and the distribution of the hyperfine induction field at the ^{57}Fe nuclei of FeSiB alloy

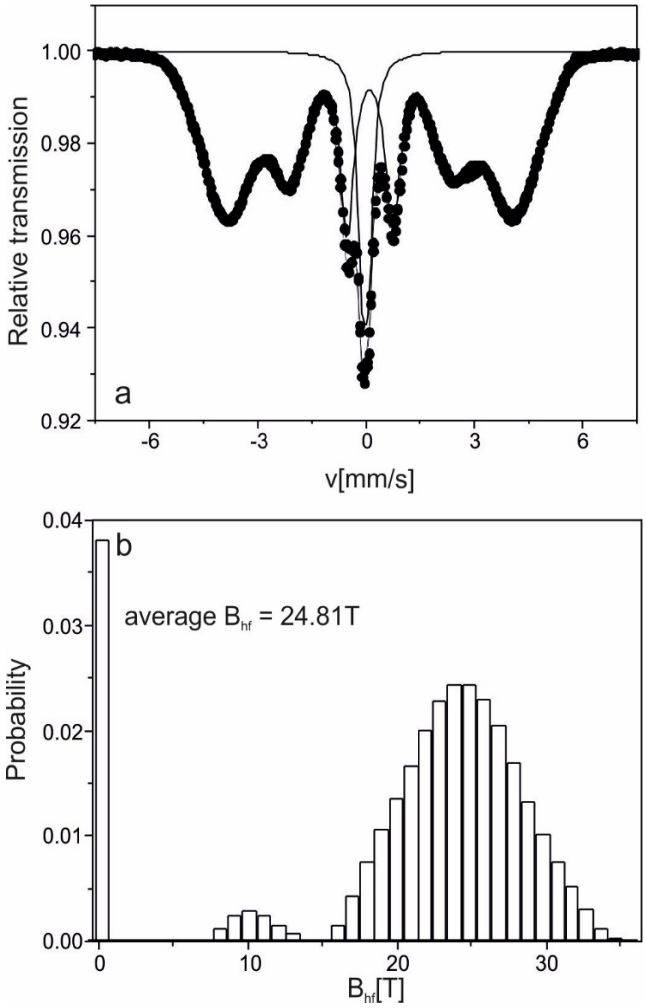

Fig. 6. The transmission Mössbauer spectrum and the distribution of the hyperfine induction field at the ^{57}Fe nuclei for FeSiBY alloy

The structure of the samples was further investigated using X-ray diffraction. In figure 7 X-ray diffraction is given together with an Rietveld analysis obtained for the investigated alloys.

Quantative Rietveld phase refinement was performed using FullProf software. Fiting parameters included: scale factor, unit cel and background parameters. For background definition a polynominal function was used (with 5 parameters). Peak shapes were described by Pseudo-Voight function. The main reason for performing Rietveld refinement was to find percentage share of visible phases. Well agreement between observed and calculated pattern was achieved (Fig. 7). The chi-squared parameter did not exceed chi^2=3.1. As can be seen on Fig. 7 two crystalline phases namely $Fe_{0.91}Si_{0.09}$ and gamma-Fe were identified. From basic cell parameters refinement it was calculated the lattice parameter 'a' for both cubic phases. The $Fe_{0.91}Si_{0.09}$ phase (space group Im-3m, no. 229) lattice a parameter was a = 0.28492 nm, similar as for pure alpha-Fe phase. The gamma-Fe (space group Fm-3m (no. 225)) lattice a parameter was refined to 0.35831 nm. Therefore it is possible, that yttrium atom entered inside unit cell becoming element of distension and stabilizing this phase. Because XRD patterns were taken from tapes surface, and the depth of X-ray penetration in metallic samples is limited, the observed XRD pattern comes more likely from sample surface only, rather than from the volume. In Fig. 8 are given the initial magnetization curves for the tested alloys. The shape of the initial magnetization curves is similar and corresponds to materials with low effective anisotropy. The contribution of the paramagnetic phase has no effect on

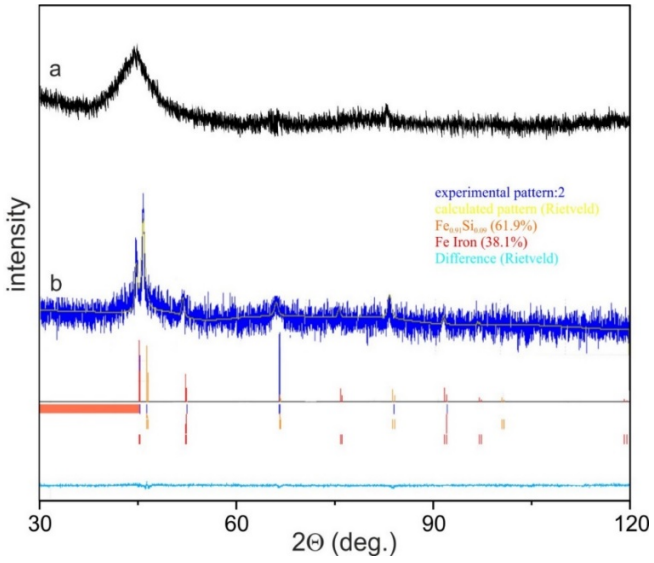

Fig. 7. X-ray diffraction patterns with Rietveld analysis obtained for the investigated alloys: a) FeSiB, b) FeSi

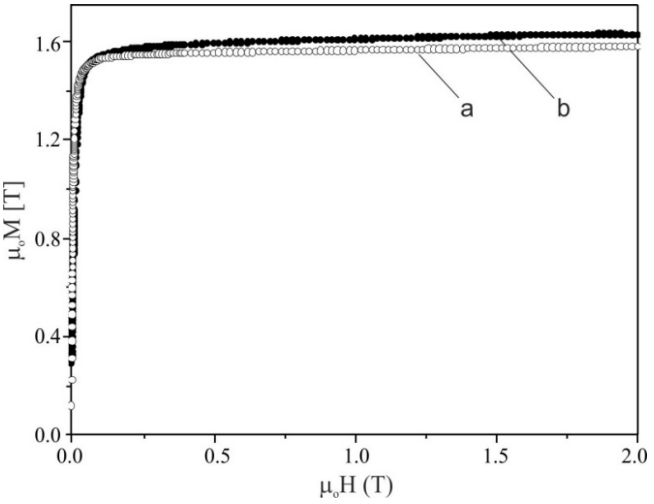

Fig. 8. Primary magnetization curves for the investigated alloys: a) FeSiB, b) FeSiBY

reducing the saturation magnetization, since it's volume fraction is small and the grain from which it is constructed is several nanometers.

4. Conclusions

Samples were fabricated using rapid cooling at a rotating copper wheel. Obtained in this manufacturing technique cooling rate may be up to 10^6 K/s. Therefore, it is possible to partially freeze the specific phases in different areas of the samples.

Samples obtained using this technology can be divided into three areas of cross section, although the obtained tapes usually had a thickness of about 35 μm. As the least variable in terms of chemical and topological order is the core of the tape, and as a subsurface layer should be considered planes to a thickness of several nanometers. Interesting in this technique is that, when forming the tape higher cooling rate is obtained on the outer side thereof, that is, the non-contact of the copper wheel. This means that even in the case of production of thin tape there is a certain temperature distribution during solidification. Additionally, this distribution is one direction heading to the surface of the copper wheel. This can cause pre-segregation of alloy components, and even lead to partial separation of the individual components having various elementary cells. In the case of rapid cooling, the freezing of a melted solution of pure iron can be observed maintaining presence of all the unit cells types (γ, δ, α). Such is situation is observed in the case of an investigated alloy. During solidification of the melt a freeze of the high-temperature phase γ–Fe occurred forming a thin film on a few nanometers with paramagnetic properties (Fig. 6). Confirmation of this result was also obtained in the surface where the only X-ray studies identified crystalline phase with fine grain: γ–Fe. An interesting fact is that the appearance of 13% paramagnetic phase had no impact on the reduction of the saturation magnetization, contrary there was quite the opposite effect. Most likely increase the magnetization of the sample with the paramagnetic phase is the result of increased structural order in terms of topological and chemical order related to an amorphous matrix. Rearrangement of atoms in the presence of a large radius Y are the reason for blocking of the atomic motion of smaller atoms over long distances and locally at the sample surface resulting from the copper wheel side what breaks the ferromagnetic interchange interactions. However, the entire volume of the alloy (excluding the surface layer) ferromagnetic interactions have strong influence on enhancing the value of saturation magnetization. The arrangement of atoms in such areas is similar to the configuration of phase α-Fe and $Fe_{0.91}Si_{0.09}$ which contribute to the growth of the magnetization.

In conclusion, it is often in the papers about the rapid cooled materials, studies of the structure and microstructure are made from the sample surface side, which can be misleading, as demonstrated in this work. It is therefore important to show existing traps in the description of the structure and properties of such alloys.

References

[1] A. Inoue, B. Shen, New Fe-based bulk glassy alloys with high saturated magnetic flux density of 1.4-1.5 T, Material Science and Engineering A 375-377 (2004) 302-306.

[2] C.H. Smith, Application of rapidly solidified soft magnetic alloys, in: H.H. Liebermann (ed.), Rapidly Solidified Alloys, Marcel Dekker, New York, 1993, 139-155.

[3] A. Inoue, J.S. Gook, Fe-based ferromagnetic glassy alloys with wide supercooled liquid region, Materials Transactions JIM 36 (1995) 1180-1183.

[4] V. Ponnambalam, S.J. Poon, G.J. Shiflet, V.M. Keppens, R. Taylor, G. Petculescu, Synthesis of iron-based bulk metallic glasses as nonfer-romagnetic amorphous steel alloys, Applied Physics Letters 83 (2003) 1131-1133.

[5] A. Inoue, T. Zhang, H. Koshiba, A. Makino, New bulk amorphous Fe-(Co, Ni)-MB (M=Zr,Hf,Nb,Ta,Mo,W) alloys with good soft magnetic properties, Journal of Applied Physic 83 (1998) 6326-6328.

[6] M. Marinescu, H. Chiriac, M. Grigoras, Magnetic properties of bulk nanocomposite permanent magnets based on NdDyFeB alloys with additions, Journal of Magnetism and Magnetic Materials 290-291 (2005) 1267-1269.

[7] W. Zhang, A. Inoue, Bulk nanocomposite permanent magnets produced by crystallization of (Fe,Co)-(Nd,Dy)-B bulk glassy alloy, Applied Physics Letters 80 (2002) 1610.

[8] A. Inou, T. Zhang, N. Nishiyama, K. Ohba, T. Masumoto, Preparation of 16 mm diameter rod of amorphous $Zr_{65}Al_{7.5}Ni_{10}Cu_{17.5}$ alloy, Materials Transactions JIM 34 (1993) 1234-1237.

[9] A. Inoue, T. Zhang, N. Nishiyama, Amorphous Zr-Al-TM (TM = Co, Ni, Cu) alloys with significant supercooled liquid region of over 100 K, Materials Transactions JIM 32 (1991) 1005-1010.

[10] A. Parker, W.L. Johnson, A highly processable metallic glass: $Zr_{41.2}Ti_{13.8}Cu_{12.5}Ni_{10}Be_{22.5}$, Applied Physics Letters 63 (1993) 2342-2344.

[11] A. Inoue, A. Takeuchi, T. Zhang, Ferromagnetic Bulk Amorphous Alloys, Metallurgical and Materials Transactions A 29 (1998) 1779-1793.

[12] A. Inoue, Bulk amorphous alloys, Trans Tech Publications, Zurich, 1998-1999.

[13] H. Izumi, H. Sunada, Y. Hayashi, T. Masumoto, Fatigue Properties of Amorphous $Ni_{75}Si_8B_{17}$ and $Co_{75}Si_{10}B_{15}$ Alloys, Journal of the Japan Institute of Metals 48 (1984) 371-377.

[14] Y. Yokoyama, N. Nishiyama, K. Fukaura, H. Sunada, A. Inoue, Rotating-beam fatigue straight of $Pd_{40}Cu_{30}Ni_{10}P_{20}$ bulk amorphous alloy, Materials Transactions JIM 40 (1999) 696-699.

[15] H.K. Lachowicz, Magnetyki amorficzne, metody wytwarzania, właściwości zastosowania techniczne, Instytut Fizyki Polskiej Akademii Nauk, Warszawa, 1983.

[16] H.S. Chen, C.E. Miller, A rapid quenching technique for the preparation of thin uniform films of amorphous solids, Review of Scientific Instruments, 1970, 411237.

[17] K. Koumoto, T. Mori, Thermoelectric nanomaterials, Materials Design and Applications, Springer Series in Materials Science 182 (2013).

[18] M. Dośpiał, M. Nabiałek, M. Szota, J. Gondro, The magnetization reversal processes of bulk (Nd, Y)-(Fe, Co)-B alloy in the as-quenched state, Archives of Metallurgy and Materials 60/3 (2015) 1587-1590.

[19] Y. Wang, X. Song, Z. Sun, X. Zhou, J. Guo, The solidification of CuCe alloys under various cooling rates, Materials-Science Poland 25 /1 (2007) 199-207 .

[20] K.S. Kim, S.G. Min, S.C. Yu, S.K. Oh, Y.C. Kim, K.Y. Kim, The large magnetocaloric effect in amorphous $Fe_{91-x}Y_xZr_9$ (x = 0, 5, 10) alloys, Journal of Magnetism and Magnetic Materials 304 (2006) e642-e644.

[21] T. Liu, Z. X. Xu, R. Z. Ma, Structural defects and internal stress field distribution in nanocrystalline $Fe_{73.5}Cu_1Nb_3Si_{13.5}B_9$, Journal of Magnetism and Magnetic Materials 152 (1996) 365-369.

[22] L. Jeziorski, M.G. Nabiałek, M. Szota, M. Dośpiał, Method of continuous casting of amorphous metallic materials based on iron, Archives of Foundry Engineering 11/4 (2011) 69-72.

[23] R.D. Fisher, D.E. Koopman, Structure softelectroless cobalt films, Journal of The Electrochemical Society 11 (1964) 263-264.

[24] A.I. Gubanov, Kvazi klassices kajateorija amorfnych ferromagnetikov, Fizika Tverdego Tela 2 (1960) p. 502 (in Russian).

[25] T. Mizushima, K. Jkarashi, A. Makino, A. Inoue, Structure and magnetic properties of bulk Fe-Al-Ga-P-C-B-Si glassy alloys in a ringed form prepared by copper mold casting, IEEE Transactions on Magnetics 35 (1999) 3361-3363.

[26] T. Itoi, A. Inoue, High-frequency permeability of (Fe, Co, Ni)$_{62}Nb_8B_{30}$ amorphous alloys with a wide supercooled liquid region, Applied Physics Letters 74 (1999) 2510-2512.

[27] Y. Yoshizawa, K. Yamauchi, S. Oguma, European Patent Application 0271657 (22.06.1988).

[28] Y. Yoshizawa, S. Oguma, K. Yamauchi, New Fe-based soft magnetic alloys composed of ultrafine grain structure, Journal of Applied Physic 64 (1998) 6044-6046.
[29] C. Han, A. Takeuchi, A. Inoue, Materials Transactions JIM 40 (1999) 42.
[30] T. Kulik, Nanokrystaliczne materiały magnetycznie miękkie otrzymane przez krystalizację szkieł metalicznych, Oficyna Wydawnicza Politechniki Warszawskiej, 1998.
[31] A. Inoue, Bulk amorphous and nanocrystalline alloys with high functional properties, Materials Science and Engineering A 304-306 (2001) 1-10.
[32] T. Kulik, The Influence of Copper, Niobium and Tantalum Additions on the Crystallization of Fe-Si-B-Based Glasses, Materials Science and Engineering A 159 (1992) 95-101.
[33] L.K. Varga, E. Bakos, E. Kisdi-Koszo, E. Zsoldos, L.F. Kiss, Time and Temperature-Dependence of Nanocrystalline Structure Formation in a Finemet-Type Amorphous Alloy, Journal of Magnetism and Magnetic Materials 133 (1994) 280-282.
[34] T. Graf, G. Hampel, J. Korus, J. Hesse, G. Herzer, Influence of Nb concentration on structure and crystallization onset of amorphous Fe(Cu,Nb)SiB finemet alloys, Nanostructural Materials 6/1-4 (1995) 469-472.
[35] M. Nabiałek, J. Zbroszczyk, W. Ciurzyńska, J. Olszewski, S. Lesz, P. Brągiel, J. Gondro, K. Sobczyk, A. Łukiewska, J. Świerczek, P. Pietrusiewicz, Microstructure, somemagnetic and mechanical properties of amorphous $Fe_{61}Co_{10}Zr_{2.5}Hf_{2.5}W_2Y_2B_{20}$ plates, Archives of Metallurgy and Materials 55(2010) 195-203.
[36] R. Li, S. Kumar, S. Ram, M. Stoica, S. Roth, J. Eckert, Crystalization and magnetic properties of $[(Fe,Co)_{0.75}Si_{0.05}B_{0.20}]_{94}$ metallic glasses, Journal of Applied Physic 42 (2009) 085006.
[37] W.M. Wang, A. Gebert, S. Roth, U. Kuehn, L. Schultz, Effect of Si on glass forming ability, thermal stability and magnetic properties of amorphous $Fe_{60}Co_8Zr_xMo_5W_2B_ySi_{25-x-y}$ alloys, Journal of Alloys and Compounds 459 (2008) 203-208.
[38] A. Makino, T. Kubota, C. Chang, M. Makabe, A. Inoue, FeSiBP bulk metallic glasses with high magnetization and excellent magnetic softness, Journal of Magnetism and Magnetic Materials 320 (2008) 2499-2503.
[39] X.D. Wang, J.Z. Jiang, S. Yi, Reversible structural relaxation and crystallization of $Zr_{62}Al_8Ni_{13}Cu_{17}$ bulk metallic glass, Journal of Non-Crystalline Solids 353 (2007) 4157-4161.
[40] S.F. Guo, Z.Y. Wu, L. Liu, Preparation and magnetic properties of FeCoHfMoBY bulk metallic glasses, Journal of Alloys and Compounds 468 (2009) 54-57.
[41] T. Kulik, H. Matyja, Effect of flash- and furnace annealing on the magnetic and mechanical properties of metallic glasses, Materials Science and Engineering A 133 (1991) 323-235.
[42] M. Nabiałek, Wytwarzanie oraz właściwości stopów amorficznych I nanokrystalicznych na bazie żelaza, Wydawnictwo Wydziału Inżynierii Procesowej, Materiałowej i Fizyki Stosowanej, Politechniki Częstochowskiej, Seria monografie nr 22, 2012.
[43] S. Takayama, Y. Oi, The analysis of casting conditions of amorphous alloys, Journal of Applied Physics 50 (1979) 4962-4965.
[44] H. Lachowicz, Amorphous Magnetic Materials, Publikacje Instytutu Fizyki Polskiej Akademii Nauk, Warszawa (1983) 30 (in Polish).